J. Webster (ed.), *Wiley Encyclopedia of Electrical and Electronics Engineering*

AIRCRAFT DYNAMICS AND CONTROL

Aircraft dynamics refers to the equations that describe how an aircraft responds to the forces and moments that act upon it. *Aircraft control* refers to the ability to move an aircraft along a desired trajectory in three-dimensional space at some desired speed. The subject is approached here in three parts. First, the equations that describe the motion of a rigid aircraft in a moving (nonquiescent) air mass are presented and discussed. Second, the applicability of these equations is demonstrated, and the topic of control synthesis is introduced through a simple control design example. The example requires only control synthesis techniques covered in a typical undergraduate engineering course on the subject and represents what has been termed a *classical* approach to aircraft control. Implementation of the resulting control system on a digital computer is discussed, and a simulation of the flight control system is presented. Third, *modern* control design approaches are discussed that involve control synthesis techniques more advanced than that of the design example. Pertinent concepts and definitions are introduced throughout.

Background

Flight control is achieved by application of appropriate forces and moments to the aircraft structure. These forces and moments can be categorized as (1) gravitational, (2) aerodynamic, and (3) propulsive. Obviously, the gravitational force in not under direct control and changes in magnitude only as the aircraft's mass changes, e.g., as fuel is expended or loads are added and shed. Aerodynamic forces and moments are created by the passage of the aircraft through the air mass. The magnitude and directions of the resultants of these latter forces and moments are modified through the action of *control effectors* such as elevators and rudders. Propulsive forces and moments are created by the particular propulsion system associated with the aircraft, for example, reciprocating, propeller-driven, turbojet-driven. In gliding flight, gravity itself provides the propulsive force. The magnitude of the propulsive forces and moments are modified by changes in thrust. In some modern combat aircraft, not only the magnitude but the direction of the propulsive force relative to the aircraft can be altered by employing what is called *thrust-vector control*.

Aerodynamic forces are primarily a function of the aircraft's speed, its altitude, and its orientation and rate of change of orientation with respect to the *relative wind*. Relative wind refers to the instantaneous direction of the air mass that an observer moving with the aircraft would measure, that is, the direction of the air mass relative to the aircraft. Thus, in a quiescent air mass, one that is not moving with respect to the earth's surface, the direction of the relative wind is simply equal and opposite to the direction of the velocity vector of the aircraft center of gravity.

In order to change the aircraft's orientation, the aerodynamic control effectors just mentioned are employed, and the magnitude and possibly the direction of the thrust force created by the propulsive system are varied. Figure 1 is a representation of the control effectors on a modern aircraft, here chosen as a tailless fighter. The control effectors in Fig. 1 are essentially devices to create aerodynamic moments about the aircraft center of gravity. The effect of these moments is to create rotational acceleration about the center of gravity

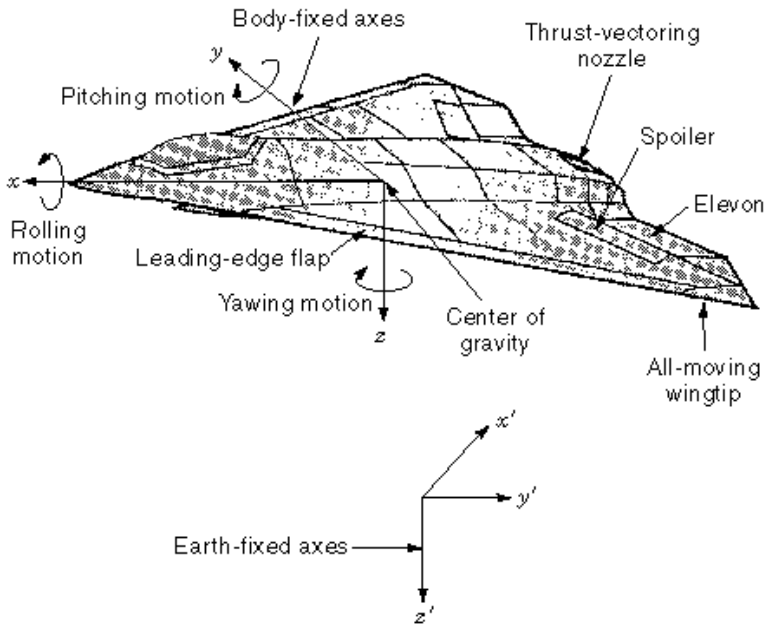

Fig. 1. Control effectors on a modern aircraft.

and hence change the orientation of the aircraft with respect to the relative wind. This, in turn, alters the total aerodynamic forces and moments acting on the aircraft. The changes in aerodynamic forces and moments created by the change in orientation are typically much larger than those created by the effectors themselves, and it is the former forces and moments that change the aircraft's trajectory and speed.

As Fig. 1 indicates, tradition has led to the description of the change in orientation of an aircraft as *pitching, rolling*, and *yawing* motions, each described by a rotation with respect to an axis system fixed in the vehicle with origin at the center of gravity. The principal aim of aircraft control is to modulate the aerodynamic and propulsive forces so as to produce the desired motion of the vehicle. In the early days of flight, this was accomplished solely by the pilot, who determined the desired trajectory and speed and, through training, moved the control surfaces by means of hand and foot controls (referred to as cockpit inceptors) so as to produce the desired results. In simplest terms, the pilot *commanded* the desired aircraft trajectory and speed, *sensed* the actual aircraft trajectory, and *actuated* the control surfaces in response to the differences in these quantities. This process constitutes the activity of a *feedback control system*. As shown in Fig. 2, much for the responsibility for feedback in the case of modern high-performance aircraft has been assumed by inanimate systems, incorporating accurate sensors and precise, powered actuators to move control effectors in a manner prescribed by a *flight control law* typically implemented on an onboard digital computer, frequently referred to as the *flight control computer*. Indeed, in most modern high-performance aircraft, the pilot is no longer directly connected to the control effectors by means of cables, pulleys, etc. Pilot commands are sent directly to the flight control computer, and the resulting system is referred to as *fly-by-wire*.

The design and implementation of an aircraft flight control system must begin with an appropriate mathematical representation or model of the dynamics of the aircraft, that is, developing the equations that describe how an aircraft responds to control effector actuation and to atmospheric disturbances such as turbulence.

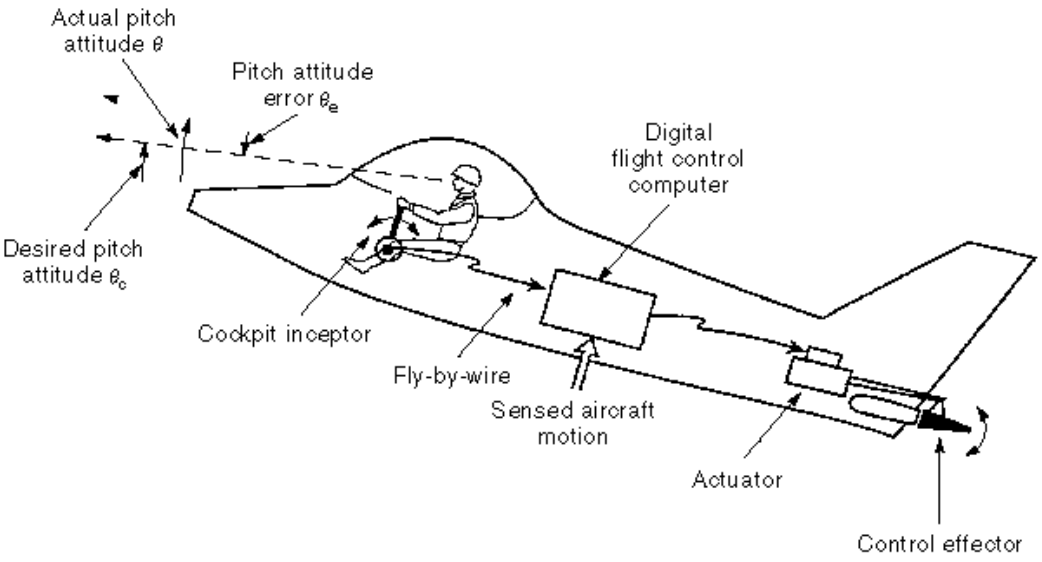

Fig. 2. Control-system elements in a modern piloted aircraft.

Mathematical Description Of The Aircraft

Body-Fixed Axis System. Referring to Fig. 1, one sees an *xyz* axis system consisting of three mutually perpendicular (orthogonal) axes with origin at the aircraft's center of gravity. These so-called *body-fixed axes* are important in the development of the mathematical model of the aircraft. As the name implies, the body-fixed axes are fixed in the aircraft body or airframe. The axis system has its origin at the aircraft center of mass, with the *xz* axes lying in the aircraft's plane of symmetry. In the equations to be presented, *stability axes* will used, wherein the x axis will be aligned with the relative wind when the aircraft is in equilibrium or "trimmed" flight.

Earth-Fixed Axis System. In addition to the body-fixed axes just defined, the description of aircraft motion and, in particular, its motion relative to the earth requires the introduction of an *earth-fixed axis system*, $x'y'z'$, also shown in Fig. 1. Traditionally, this axis system has its z' axis directed toward the center of the earth, with the position of its origin and x' axis direction up to the analyst's discretion. For example, the origin may be assumed to lie at a particular geographical location on or above the earth's surface with the x' axis pointed in the direction of magnetic north.

Equations of Motion.

Equations Expressed in Earth-Fixed Coordinates. The equations that follow are similar to those to be found in any standard text on the subject, for example, Etkin (1), Nelson (2), or Schmidt (3). In deriving these equations, it is typically assumed that the aircraft is a rigid body, that is, that the linear separation of any two particles in the aircraft is constant. Like the assumption of symmetry, this one is never actually true. It is justified in many applications, however. In simplest form, the aircraft equations of motion consist of a pair of vector equations relating the vector sum of the forces and moments acting on the aircraft and the linear and angular accelerations which they produce. These equations are

$$\boldsymbol{F} = m\frac{d\,\boldsymbol{v}_c}{dt}, \qquad \boldsymbol{G} = \frac{d\,\boldsymbol{h}}{dt} \tag{1}$$

where

$\boldsymbol{F}$ = vector sum of all the external forces acting on the aircraft with this vector acting through the aircraft's center of gravity

m = total mass of the aircraft

$\boldsymbol{v}_c$ = instantaneous velocity of the aircraft's center of gravity

d/dt = derivative evaluated in the earth-fixed axis system

$\boldsymbol{G}$ = vector sum of all the external moments acting on the aircraft

$\boldsymbol{h}$ = vector sum of the instantaneous angular momentum vectors of each particle of the aircraft, with respect to the aircraft center of mass.

All the quantities just defined are, in general, functions of time. For the purposes of designing aircraft control systems, however, the mass of the aircraft is usually assumed to be constant.

Equations (1) are vector equations, that is, they describe vectors that are uniquely specified by their magnitude and direction. There is considerable benefit in expressing the vectors in the body-fixed axis system that has just been described. As will be seen, one such benefit lies in the simplification of the angular momentum vector $\boldsymbol{h}$.

Position and Orientation of the Aircraft. In order to be able to prescribe a desired trajectory for the aircraft center of mass, it is necessary to determine the position and orientation of the aircraft (or equivalently its body-fixed axis system) relative to the earth-fixed reference frame or axis system. Accomplishing this requires the introduction and definition of three angles referred to as the *Euler angles*. These angles can be used to uniquely prescribe the orientation of the body-fixed axes relative to the earth-fixed axes through three ordered rotations as shown in Fig. 3. Note that the order of the rotations Ψ, Θ, Φ is essential to the definition of the Euler angles.

Equations Expressed in Body-Fixed Coordinates. The vectors $\boldsymbol{F}$, $\boldsymbol{v}_c$, $\boldsymbol{G}$, and $\boldsymbol{h}$ can be conveniently expressed as components in the body-fixed xyz axes of Fig. 1 as follows:

$$\begin{aligned}\boldsymbol{F} = F_x\,\boldsymbol{i} + F_y\boldsymbol{j} + F_z\,\boldsymbol{k} &= (X - mg\,\sin\Theta)\boldsymbol{i} \\ &+ (Y + mg\,\cos\Theta\,\sin\Phi)\boldsymbol{j} + (Z + mg\,\cos\Theta\,\cos\Phi)\boldsymbol{k}\end{aligned} \tag{2}$$

$$\boldsymbol{v} = U\boldsymbol{i} + V\boldsymbol{j} + W\boldsymbol{k} \tag{3}$$

$$\boldsymbol{G} = L\boldsymbol{i} + M\boldsymbol{j} + N\boldsymbol{k} \tag{4}$$

$$\boldsymbol{h} = h_x\,\boldsymbol{i} + h_y\boldsymbol{j} + h_z\,\boldsymbol{k} \tag{5}$$

where $\boldsymbol{i}$,$\boldsymbol{j}$,$\boldsymbol{k}$ represent unit vectors parallel to the x, y, and z body-fixed axes and where X, Y, and Z represent the components of the aerodynamic and propulsive forces alone, with the contribution of the gravitational forces now included in such terms as $-mg\,\sin\Theta$. The scalar quantities L, M, and N are usually referred to as the *rolling moment*, *pitching moment*, and *yawing moment*, respectively.

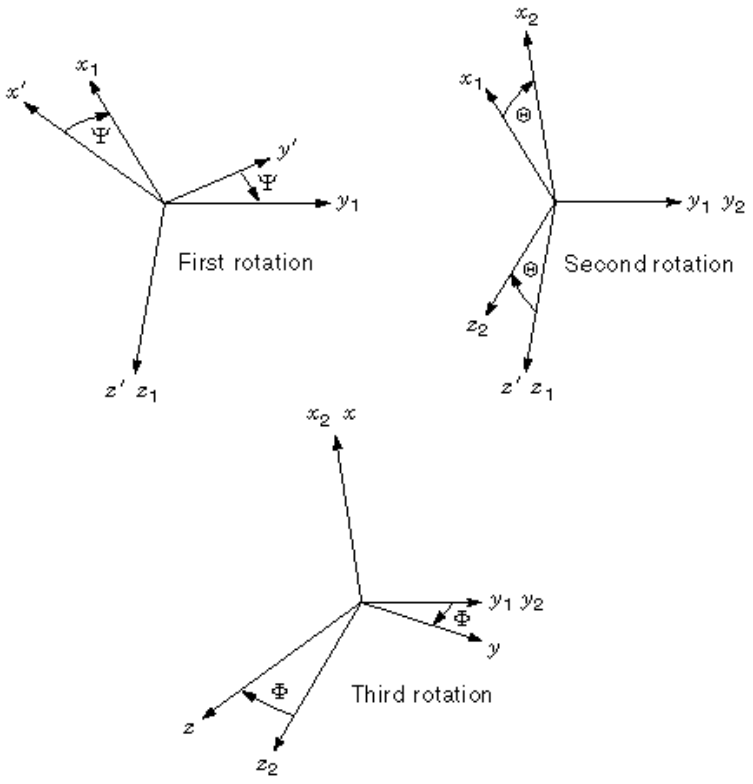

Fig. 3. The Euler angles.

The angular velocity of the aircraft as evaluated in the earth-fixed axis system must also be introduced and defined. This quantity is also a vector, denoted ω. Expressed in the body-fixed axes, it becomes

$$\boldsymbol{\omega} = P\boldsymbol{i} + Q\boldsymbol{j} + R\boldsymbol{k} \tag{6}$$

The scalar quantities P, Q, and R are typically referred to as the roll rate, pitch rate, and yaw rate, respectively.

The components of the aircraft's instantaneous angular velocity defined in Eq. (6) can be related to the time rate of change of the Euler angles as

$$\begin{aligned}
\dot{\Theta} &= Q\cos\Phi - R\sin\Phi \\
\dot{\Phi} &= P + Q\sin\Phi\tan\Theta + R\cos\Phi\tan\Theta \\
\dot{\Psi} &= Q\sin\Phi\sec\Theta + R\cos\Phi\sec\Theta
\end{aligned} \tag{7}$$

Finally, the scalar components of $\boldsymbol{h}$ can be expressed in terms of fundamental geometric properties of the aircraft as

$$\begin{aligned} h_x &= PI_{xx} - QI_{xy} - RI_{xz} \\ h_y &= -PI_{xy} + QI_{yy} - RI_{yz} \\ h_z &= -PI_{xz} - QI_{yz} + RI_{zz} \end{aligned} \tag{8}$$

where the subscripted I symbols represent moments and products of inertia. The choice of body-fixed axes in which to express the vectors associated with aircraft motion means that the moments and products of inertia in Eq. (8) are constants rather than functions of time, a considerable simplification.

With the Euler angles defined, expressions for the velocity components of the aircraft center of gravity can now be expressed in the earth-fixed axis system as

$$\begin{aligned} \dot{x}' &= U\cos\Theta\cos\Psi + V(\sin\Phi\sin\Theta\cos\Psi - \cos\Phi\sin\Psi) \\ &\quad + W(\cos\Phi\sin\Theta\cos\Psi + \sin\Phi\sin\Psi) \\ \dot{y}' &= U\cos\Theta\sin\Psi + V(\sin\Phi\sin\Theta\sin\Psi + \cos\Phi\cos\Psi) \\ &\quad + W(\cos\Phi\sin\Theta\sin\Psi - \sin\Phi\cos\Psi) \\ \dot{z}' &= -U\sin\Theta + V\sin\Phi\cos\Theta + W\cos\Phi\cos\Theta \end{aligned} \tag{9}$$

When integrated over time, the differential equations in Eq. (9) yield the position of the aircraft relative to the earth-fixed axes, i.e., the *aircraft trajectory*.

The right-hand sides of Eqs. (1) can be made more tractable by evaluating the derivatives in the body-fixed axis system:

$$\boldsymbol{F} = m\left[\frac{d\boldsymbol{v}_c}{dt}\right]_{\text{body}} + m(\boldsymbol{\omega}\times\boldsymbol{v}_c), \qquad \boldsymbol{G} = \left[\frac{d\boldsymbol{h}}{dt}\right]_{\text{body}} + \boldsymbol{\omega}\times\boldsymbol{h} \tag{10}$$

where $[\cdot]_{\text{body}}$ indicates a derivative evaluated in the body-fixed axis system.

Complete Mathematical Model. The complete mathematical model of the aircraft can now be presented. Some algebraic manipulation has been employed to present the equations in a form in which only first derivatives are involved and they appear on the left-hand side of the equations, i.e., a *state-space* description:

$$\dot{U} = \frac{X}{m} - QW + RV - g\sin\Theta \tag{11a}$$

$$\dot{V} = \frac{Y}{m} - RU + PW + g\cos\Theta\sin\Phi \tag{11b}$$

$$\dot{W} = \frac{Z}{m} - PV + QU + g\cos\Theta\cos\Phi \tag{11c}$$

$$\dot{P} = \frac{1}{I_{xx}\left(1 - I_{xz}^2/I_{xx}I_{zz}\right)}\left[L + \frac{I_{xz}}{I_{zz}}[N + PQ(I_{xx} - I_{yy} + I_{zz})] + QR\left(I_{yy} - I_{zz} - \frac{I_{xz}^2}{I_{zz}}\right)\right] \tag{11d}$$

$$\dot{Q} = \frac{1}{I_{yy}}[M + RP(I_{zz} - I_{xx}) + I_{xz}(R^2 - P^2)] \tag{11e}$$

$$\dot{R} = \frac{1}{I_{zz}\left(1 - I_{xz}^2/I_{xx}I_{zz}\right)}\left[N + \frac{I_{xz}}{I_{xx}}[L + QR(I_{yy} - I_{zz} - I_{xx})] + PQ\left(\frac{I_{xz}^2}{I_{xx}} + I_{xx} - I_{yy}\right)\right] \tag{11f}$$

$$\dot{\Theta} = Q\cos\Phi - R\sin\Phi \tag{11g}$$

$$\dot{\Phi} = P + Q\sin\Phi\tan\Theta + R\cos\Phi\tan\Theta \tag{11h}$$

$$\dot{\Psi} = Q\sin\Phi\sec\Theta + R\cos\Phi\sec\Theta \tag{11i}$$

$$\dot{x}' = U\cos\Theta\cos\Psi + V(\sin\Phi\sin\Theta\cos\Psi - \cos\Phi\sin\Psi) + W(\cos\Phi\sin\Theta\cos\Psi + \sin\Phi\sin\Psi) \tag{11j}$$

$$\dot{y}' = U\cos\Theta\sin\Psi + V(\sin\Phi\sin\Theta\sin\Psi + \cos\Phi\cos\Psi) + W(\cos\Phi\sin\Theta\sin\Psi - \sin\Phi\cos\Psi) \tag{11k}$$

$$\dot{z}' = -U\sin\Theta + V\sin\Phi\cos\Theta + W\cos\Phi\cos\Theta \tag{11l}$$

Equations (11) constitute a set of nonlinear ordinary differential equations. Unfortunately, most of the classical feedback control techniques require the object of control to be described by linear ordinary differential equations. Thus, Eqs. (11) must be linearized. (This restriction will be removed when modern control synthesis techniques are discussed.) The linearization will allow the unknown forces and moments on the right-hand sides of Eqs. (10) to be described in terms of *stability derivatives* that can be obtained from fundamental aerodynamic theory, computational aerodynamics, and experiment (e.g., wind-tunnel testing).

Linearization.

Small-Disturbance Theory. Linearization of the Eqs. (11) begins with the assumption of an *equilibrium condition*, or *equilibrium point*, about which *small-disturbance motion* of the aircraft is assumed to occur. An equilibrium condition can be defined as one in which the aircraft exhibits constant linear and angular momentum. Perturbation variables are then introduced. This means that each time-dependent variable appearing in Eqs. (11) is represented by the sum of its value at the equilibrium condition and a small perturbation value. The perturbation notation can be summarized as follows:

$$U = u_0 + u, \qquad P = p_0 + p, \qquad \Theta = \theta_0 + \theta, \qquad \text{etc.} \tag{12a}$$

$$X = X_0 + \Delta X, \qquad L = L_0 + \Delta L, \text{ etc.} \tag{12b}$$

$$\delta_a = \delta_{a_0} + \Delta\delta_a, \qquad \text{etc.} \tag{12c}$$

With these relations, Eqs. (11) can be linearized using small disturbance theory. Finally, the definition of the body-fixed axis system as a set of *stability axes* and the definition of the equilibrium flight condition as one of steady, wings-level flight with $\boldsymbol{v}_c$ in the plane of symmetry means that

$$v_0 = w_0 = p_0 = q_0 = r_0 = \phi_0 = 0. \tag{13}$$

Linear Air Reactions—Stability Derivatives. To retain the desired linear form of the equations of motion, the perturbed aerodynamic forces and moments, ΔX, ΔL, etc., must be expressed as *linear* functions of the remaining perturbation values and their derivatives. This is traditionally accomplished through the assumption of *linear air reactions*. For example, the x component of the aerodynamic and propulsive force is expressed as

$$X = X_0 + \Delta X = X_0 + \left[\frac{\partial X}{\partial u}\right]_0 u + \left[\frac{\partial X}{\partial \dot{u}}\right]_0 \dot{u} + \cdots + \left[\frac{\partial X}{\partial \Delta\delta_a}\right] \Delta\delta_a + \cdots \tag{14}$$

where the subscript 0 means that the derivative is evaluated at the equilibrium condition. The inclusion of all perturbation values and derivatives on the right-hand side of Eq. (14) implies an infinite series. Fortunately, experience has shown that only a few such terms need be retained to accurately describe the aerodynamic force X.

On substituting expressions such as Eq. (14) into the linearized form of 11, a set of *linear ordinary differential equations* results. Mass and moment-of-inertia terms are typically subsumed into the linear air reaction terms, as, for example,

$$\begin{aligned} \left[\frac{\partial X}{\partial u}\right]_0 &\rightarrow \frac{1}{m}\left[\frac{\partial X}{\partial u}\right]_0 = X_u \\ \left[\frac{\partial L}{\partial p}\right]_0 &\rightarrow \frac{1}{I_{xx}}\left[\frac{\partial L}{\partial p}\right]_0 = L_p \end{aligned} \tag{15}$$

The quantities X_u and L_p are referred to as *mass- and moment-normalized stability derivatives*, and simply as *stability derivatives* in what follows. The values of the stability derivatives are a function of the

aircraft configuration and the flight condition, the latter being essentially specified by the Mach number and altitude where the equilibrium condition is defined.

Separation of the Equations. In reviewing the linearized equations, it becomes apparent that the equations separate somewhat naturally into two groups, the so-called *longitudinal* and *lateral-directional* equations. The reader should note that these equations have been simplified by ignoring certain stability derivatives that are typically small. For complete equations see any of the aircraft stability and control texts in the bibliography.

Longitudinal Equations.

$$
\begin{aligned}
\dot{u} &= X_u u + X_w w - (g \cos \theta_0)\theta + \sum_{i=1}^{n} X_{\delta_i} \Delta\delta_i \\
\dot{w} &= \frac{Z_u}{1 - Z_{\dot{w}}} u + \frac{Z_w}{1 - Z_{\dot{w}}} w + \frac{Z_q + u_0}{1 - Z_{\dot{w}}} q - \frac{g \sin \theta_0}{1 - Z_{\dot{w}}} \theta + \frac{1}{1 - Z_{\dot{w}}} \sum_{i=1}^{n} Z_{\delta_i} \Delta\delta_i \\
\dot{q} &= \left(M_u + \frac{M_{\dot{w}} Z_u}{1 - Z_{\dot{w}}} \right) u + \left(M_w + \frac{M_{\dot{w}} Z_w}{1 - Z_{\dot{w}}} \right) w + \left(M_q + \frac{M_{\dot{w}} (Z_q + u_0)}{1 - Z_{\dot{w}}} \right) q \\
&\quad - \frac{M_{\dot{w}} g \sin \theta_0}{1 - Z_{\dot{w}}} \theta + \frac{M_{\dot{w}}}{1 - Z_{\dot{w}}} \sum_{i=1}^{n} Z_{\delta_i} \Delta\delta_i + \sum_{i=1}^{n} M_{\delta_i} \Delta\delta_i \\
\dot{\theta} &= q \\
\dot{x}' &= (u_0 + u) \cos \theta_0 + w \sin \theta_0 - u_0 \theta \sin \theta_0 \\
\dot{z}' &= -(u_0 + u) \sin \theta_0 + w \cos \theta_0 - u_0 \theta \cos \theta_0
\end{aligned}
\tag{16}
$$

The n appearing in the summations represents the number of aerodynamic control effectors being employed. Also note that $\dot{x}'$ and $\dot{z}'$ are not perturbation quantities, as they represent velocity components of the aircraft's center of mass, expressed in earth-fixed axes.

Lateral-Directional Equations.

$$
\begin{aligned}
\dot{v} &= Y_v v + Y_p p + (Y_r - u_0) r + (g \cos \theta_0)\theta + \sum_{i=1}^{n} Y_{\delta_i} \Delta\delta_i \\
\dot{p} &= L'_v v + L'_p p + L'_r r + \sum_{i=1}^{n} L'_{\delta_i} \Delta\delta_i \\
\dot{r} &= N'_v v + N'_p p + N'_r r + \sum_{i=1}^{n} N'_{\delta_i} \Delta\delta_i \\
\dot{\phi} &= p + r \tan \theta_0 \\
\dot{\psi} &= r \sec \theta_0 \\
\dot{y}' &= u_0 \psi \cos \theta_0 + v
\end{aligned}
\tag{17}
$$

Again, $\dot{y}'$ does not represent a perturbation quantity. The so-called *prime stability derivatives* appearing in Eq. (17) are introduced for notational convenience and are defined as

$$L'_{()} = \frac{L_{()}}{1 - I_{xz}^2/I_{xx}I_{zz}} + \frac{I_{xz}}{I_{xx}} \frac{N_{()}}{1 - I_{xz}^2/I_{xx}I_{zz}}$$
$$N'_{()} = \frac{I_{xz}}{I_{zz}} \frac{L_{()}}{1 - I_{xz}^2/I_{xx}I_{zz}} + \frac{N_{()}}{1 - I_{xz}^2/I_{xx}I_{zz}} \tag{18}$$

Atmospheric Disturbances. The most influential of all disturbances acting upon an aircraft are those due to atmospheric turbulence. Turbulence can be defined as a particular type of nonquiescent atmosphere in which rapid fluctuations of wind velocity and direction occur. An introductory treatment of this phenomenon and the manner in which it is modeled is given by Hess (4). For the purposes of this exposition, turbulence will be modeled in its simplest form. It will be assumed that the aircraft can encounter three one-dimensional turbulence velocity fields, wherein the air-mass velocity has three components u_g, w_g, and w_g parallel to the aircraft's x, y, and z body axes in the equilibrium condition. Figure 4 indicates these three velocity fields. The amplitude of each component will vary with time, but is assumed invariant over the length of the aircraft and is equal to the amplitude experienced at the aircraft's center of gravity.

Equations (16) and (17) can be modified to accommodate this simple turbulence model by realizing that:

(1) The aircraft will see a relative wind with perturbation components $u - u_g$, $v - v_g$, and $w - w_g$.
(2) The effects of this simplified turbulence representation on the dynamics of the aircraft can be approximated by modifying the aerodynamic (as opposed to the inertial) terms in Eqs. (16) and (17) so that they contain the factors $u - u_g$, $v - v_g$, and $w - w_g$ rather than simply u, v, and w

This has been done in the equations below:

$$\dot{u} = X_u u + X_w w - (g \cos \theta_0)\theta + \sum_{i=1}^{n} X_{\delta_i} \Delta\delta_i - X_u u_g - X_w w_g \tag{19a}$$

$$\dot{w} = \frac{Z_u}{1 - Z_{\dot{w}}} u + \frac{Z_w}{1 - Z_{\dot{w}}} w + \frac{Z_q + u_0}{1 - Z_{\dot{w}}} q - \frac{g \sin \theta_0}{1 - Z_{\dot{w}}} \theta$$
$$+ \frac{1}{1 - Z_{\dot{w}}} \sum_{i=1}^{n} Z_{\delta_i} \Delta\delta_i - \frac{Z_u}{1 - Z_{\dot{w}}} u_g - \frac{Z_w}{1 - Z_{\dot{w}}} w_g \tag{19b}$$

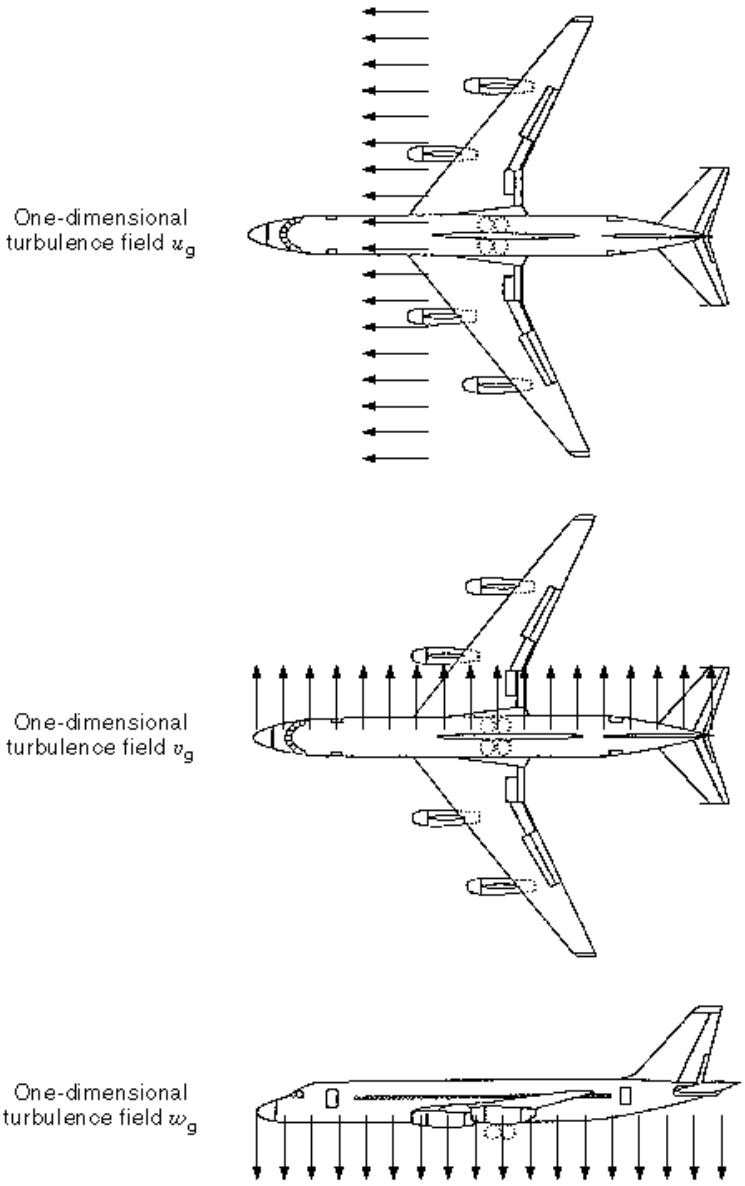

Fig. 4. Simplified representation of three one-dimensional turbulence fields.

$$\dot{q} = \left(M_u + \frac{M_{\dot{w}} Z_u}{1 - Z_{\dot{w}}}\right) u + \left(M_w + \frac{M_{\dot{w}} Z_w}{1 - Z_{\dot{w}}}\right) w + \left(M_q + \frac{M_{\dot{w}}(Z_q + u_0)}{1 - Z_{\dot{w}}}\right) q$$
$$- \frac{M_{\dot{w}} g \sin \theta_0}{1 - Z_{\dot{w}}} \theta + \frac{M_{\dot{w}}}{1 - Z_{\dot{w}}} \sum_{i=1}^{n} Z_{\delta_i} \Delta\delta_i + \sum_{i=1}^{n} M_{\delta_i} \Delta\delta_i$$
$$- \left(M_u + \frac{M_{\dot{w}} Z_u}{1 - Z_{\dot{w}}}\right) u_g - \left(M_w + \frac{M_{\dot{w}} Z_w}{1 - Z_{\dot{w}}}\right) w_g \tag{19c}$$

$$\dot{\theta} = q \tag{19d}$$

$$\dot{x}' = (u_0 + u)\cos\theta_0 + w\sin\theta_0 - u_0\theta\sin\theta_0 \tag{19e}$$

$$\dot{z}' = -(u_0 + u)\sin\theta_0 + w\cos\theta_0 - u_0\theta\cos\theta_0 \tag{19f}$$

$$\dot{v} = Y_v v + Y_p p + (Y_r - u_0)r + (g\cos\theta_0)\theta + \sum_{i=a}^{n} Y_{\delta_i}\,\Delta\delta_i - Y_v v_g \tag{20a}$$

$$\dot{p} = L'_v v + L'_p p + L'_r r + \sum_{i=a}^{n} L'_{\delta_i}\,\Delta\delta_i - L'_v v_g \tag{20b}$$

$$\dot{r} = N'_v v + N'_p p + N'_r r + \sum_{i=a}^{n} N'_{\delta_i}\,\Delta\delta_i - N'_v v_g \tag{20c}$$

$$\dot{\phi} = p + r\tan\theta_0 \tag{20d}$$

$$\dot{\psi} = r\sec\theta_0 \tag{20e}$$

$$\dot{y}' = u_0\psi\cos\theta_0 + v \tag{20f}$$

Both sets of Eqs. (19) and (20a) can be conveniently described in state-space format as

$$\begin{aligned} \dot{\boldsymbol{x}}(t) &= \boldsymbol{A}\boldsymbol{x}(t) + \boldsymbol{B}\boldsymbol{\delta}(t) + \boldsymbol{E}\boldsymbol{\gamma}(t) \\ \boldsymbol{y}(t) &= \boldsymbol{C}\boldsymbol{x}(t) + \boldsymbol{D}\boldsymbol{\delta}(t) \end{aligned} \tag{21}$$

where, for example, in the longitudinal equations,

$$\begin{aligned} \boldsymbol{x}(t) &= \{u(t),\ w(t), q(t), \theta(t), x'(t), z'(t)\}^{\mathrm{T}} \\ \boldsymbol{\delta}(t) &= \{\Delta\delta_1(t), \ldots, \Delta\delta_n(t)\}^{\mathrm{T}} \\ \boldsymbol{\gamma}(t) &= \{u_g(t), w_g(t)\}^{\mathrm{T}} \\ \boldsymbol{y}(t) &= \{\theta(t), u(t), z'_0 - z'(t)\}^{\mathrm{T}} \end{aligned} \tag{22}$$

Applicability of the Mathematical Model. Although the linearized mathematical model just developed was introduced in terms of a normally configured, fixed-wing aircraft in wing-borne forward flight, it is also applicable to other configurations, e.g., helicopters, vertical-take off and - landing aircraft, etc. Examples of applications to such vehicles can be found in McRuer, Ashkenas, and Graham (5), Heffley et al. (6), and Tischler (7). The assumptions leading to the development of the linearized aircraft equations of motion would appear to significantly restrict their utility in control-system design. In particular, the assumption of small perturbation motion about an equilibrium condition of steady, wings-level flight would, of itself, seem to be frequently violated in an aircraft's operational envelope. With the exception of large-amplitude maneuvering, however, such violations, when they do occur, typically have only a minor effect upon the utility of the equations for control-system design. One significant reason for this is that feedback itself ameliorates the effects of errors or changes in the model of the aircraft being controlled.

Aeroelasticity. The mathematical model just developed can be expanded to encompass the phenomenon of *aeroelasticity*, i.e., the inclusion of aircraft structural flexibility in the equations of motion. Aeroelasticity derives its name from the interaction of aerodynamic forces and the flexible structure. For example, structural flexibility is important in proposed supersonic passenger aircraft, where efficient, low-drag designs dictate light structures and long, slender fuselage shapes. In situations in which the flexibility of the aircraft cannot be ignored, the linear equations of motion are augmented with additional states or dependent variables, each of which is associated with a fundamental or natural *structural mode* of motion. These oscillatory structural modes are typically defined using *finite-element* analysis techniques. The aerodynamic effects of structural flexibility can be handled in a number of ways, perhaps the simplest being the application of *aerodynamic strip theory*. Waszak and Schmidt (8) provide a thorough introductory treatment of this approach, including an illustrative example. The frequencies of the structural modes are typically well above the bandwidths of the control loops that define the flight control system.

The Laplace Transform And Transfer Function

The state-space form of the equations of motion, [Eqs. (21)], can be Laplace transformed as

$$\begin{aligned} s\boldsymbol{X}(s) &= \boldsymbol{A}\boldsymbol{X}(s) + \boldsymbol{B}\boldsymbol{\Delta}(s) + \boldsymbol{E}\boldsymbol{\Gamma}(s) \\ \boldsymbol{Y}(s) &= \boldsymbol{C}\boldsymbol{X}(s) + \boldsymbol{D}\boldsymbol{\Delta}(s) \end{aligned} \tag{23}$$

where s denotes the Laplace variable and, for example,

$$\boldsymbol{X}(s) = \int_0^\infty \mathbf{x}(t)e^{-st}\,dt \tag{24}$$

the Laplace transform of the vector $\boldsymbol{x}(t)$. Simple matrix manipulation of Eq. (23) leads to

$$\boldsymbol{Y}(s) = [\boldsymbol{C}(s\boldsymbol{I} - \boldsymbol{A})^{-1}\boldsymbol{B} + \boldsymbol{D}]\boldsymbol{\Delta}(s) + \boldsymbol{C}(S\boldsymbol{I} - \boldsymbol{A})^{-1}\boldsymbol{E}\,\Gamma(s) = \boldsymbol{G}(s)\boldsymbol{\Delta}(s) + \boldsymbol{H}(s)\boldsymbol{\Gamma}(s) \tag{25}$$

where $\boldsymbol{G}(s)$ and $\boldsymbol{H}(s)$ denote *transfer-function matrices*. The element in the ith row and jth column of $\boldsymbol{G}(s)$ is the transfer function between the ith output variable and the jth input, and the element in the ith row and jth column of $\boldsymbol{H}(s)$ is the transfer function between the ith output variable and the jth turbulence input. These transfer-function elements describe the relationship between inputs (or disturbances) and outputs. For

example, given the state and output descriptions of Eq. (22), we have

$$g_{1,1}(s) = \frac{\theta}{\Delta\delta_1}(s) = \frac{a_m s^m + \cdots + a_0}{b_n s^n + \cdots + b_0} \tag{26}$$

where θ is the aircraft pitch attitude (an Euler angle) and $\Delta\delta_1$ is a particular control input, perhaps the elevon input in the aircraft of Fig. 1. The roots of the numerator and denominator polynomials on the right-hand sides of Eq. (13) are referred to as the *zeros* and *poles* of the transfer function, respectively (9). In the absence of other inputs, the time response $\theta(t)$ to the control actuation $\Delta\delta_1(t)$ can then be obtained as

$$\theta(t) = \mathscr{L}^{-1}\left(\frac{\theta}{\Delta\delta_1}(s)\ \Delta\delta_1(s)\right) \tag{27}$$

where $\mathscr{L}^{-1}$ represents the inverse Laplace transform. Stability (i.e., bounded responses to bounded inputs) requires that the poles of the transfer function $g_{11}(s)$ lie in the left half of the complex s plane. There is a fundamental, or natural, *mode of motion* associated with each real pole and each pair of complex conjugate poles of the $g_{11}(s)$. The actual response to a control actuation is a superposition of these fundamental modes. The zeros of the transfer function determine the extent to which each mode enters into the response of each output variable.

The elements of the matrices $\boldsymbol{A}$ and $\boldsymbol{B}$ of Eqs. (21) are functions of the stability derivatives and the inertial properties of the aircraft. Indeed, the name "stability derivatives" derives from the fact that the values of these parameters determine whether the poles of the aircraft transfer functions lie in the left half of the complex s plane. The earliest use of feedback in flight control systems was to artificially augment the values of specified derivatives and in doing so improve the stability of the aircraft. Such systems were referred to as *artificial stability systems* or *stability augmentation systems* (5).

Control-System Architecture

For manual, piloted control, the architecture of the flight control system itself derives from the nature of the vehicle dynamics and the necessity of the aircraft meeting *handling qualities* requirements. Handling qualities can be defined as those qualities or characteristics of an aircraft that govern the ease and precision with which a pilot is able to perform the tasks required in support of an aircraft role (10). Specifications on vehicle handling qualities are stated in terms of modal characteristics (e.g., the damping required on specific longitudinal and lateral modes of motion) and of the characteristics of the Bode plots associated with pilot-input–vehicle-output response pairs (e.g, Ref. 11, Chap. 4). Thus, the vehicle response variables selected for feedback and the architecture of the control system are typically chosen to

(1) Provide independent control of vehicle Euler angles Θ, Φ, yaw rate r, and speed $|\boldsymbol{v}_c|$ via piloted inputs from cockpit inceptors, all with satisfactory handling qualities
(2) Force the vehicle velocity vector to remain within the xz plane of the aircraft's body axes

While the prescription just outlined is admittedly an oversimplified generalization, the basic tenets implied are quite powerful and cover a wide range of flight control applications. The importance of control of Θ, and r revolves around the ability of such feedback to improve the absolute and relative stability of the vehicle

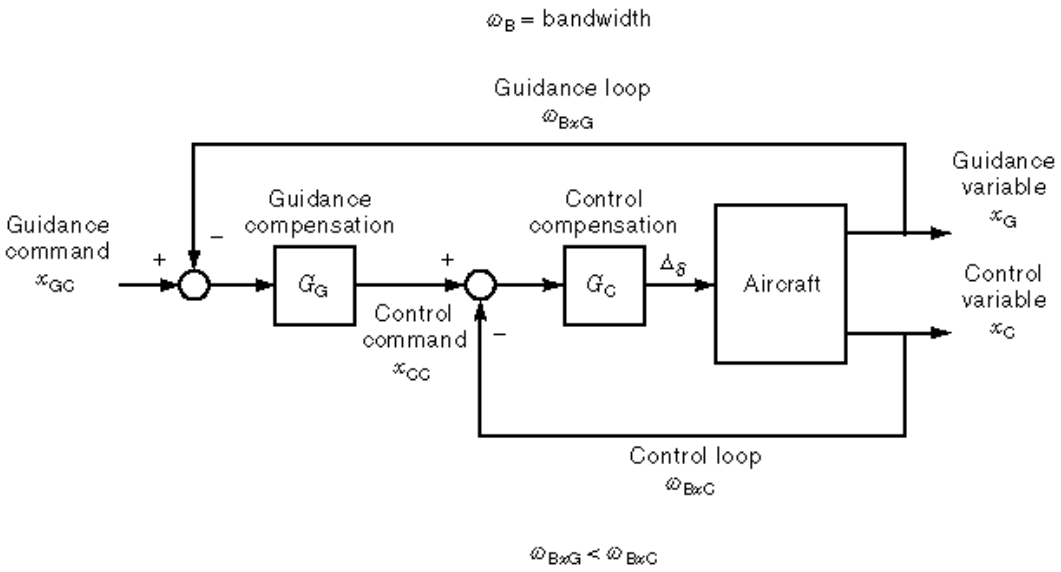

Fig. 5. Guidance- and control-loop structure typical of flight control systems.

motion. Control of the Euler angle Φ provides the primary means for trajectory modification in the horizontal plane.

In forcing an aircraft to follow a desired trajectory, outer, *guidance loops* are employed. The inner loops providing control of Euler angles and their derivatives and the outer guidance loops providing control of linear velocity and (sometimes) position are characterized by different *bandwidths*, as indicated by $\omega_{B(\cdot)}$ in the nested loop structure of Fig. 5. This nested structure is common to most flight control designs. The bandwidth specifies the maximum frequency of a sinusoidal input that can be expected to be reproduced with reasonable fidelity at the system output. A more precise definition will be given shortly. As Fig. 5 indicates, inner loops have higher bandwidths than outer loops. Outer guidance loops with lower bandwidths are then closed about the inner loops. The sensor requirements in terms of signal-to-noise ratios for the outer guidance loops are less demanding than those for the inner control loops.

Trajectory Optimization

With a control system like that just outlined in operation, an aircraft can be forced to follow a desired trajectory in three-dimensional space at some desired speed. In terms of mission effectiveness or economy some trajectories can be considered more desirable than others. For example, consider the fighter aircraft of Fig. 1 in a combat situation. To avoid an adversary the pilot must change heading (Euler angle Ψ) by 180° as quickly as possible. The question is: What trajectory and speed profile will allow this heading change to occur in minimum time? Next consider a large passenger aircraft such as that shown in Fig. 4. To minimize ticket costs it is necessary to minimize fuel consumption. The question now is: What trajectory and speed profile from departure point *A* to destination point *B* will result in minimum fuel consumption? The answers to these questions involves the discipline of *trajectory optimization*. The mathematical tools involved are those of the calculus of variations. The equations describing the aircraft motion are typically simpler than those just derived. The aircraft is represented as a point mass, upon which act the gravitational, aerodynamic, and propulsive forces.

Moment equations are not involved. The aerodynamic forces are considered nonlinear functions of the aircraft's orientation with respect to the relative wind. The texts of Bryson and Ho (12) and Stengel (13) provide excellent treatments of these problems.

Control-System Design—A Classical Approach

As has been mentioned in the preceding discussion, aircraft trajectory control is achieved using feedback either through the action of a human pilot or through the combination of a human pilot and a feedback control system or through feedback control alone (an *autopilot*). An instructive starting point for a discussion of aircraft control design is the so-called *classical* approach using fundamental analysis and synthesis tools such as the Laplace transform and Bode diagram in a process referred to as *loop shaping*. The Bode diagram is a plot of the following functions:

$$\begin{array}{l} 20\ \log_{10} \mid g_{ij}(s) \mid_{s=j\omega}\ \text{versus}\ \log\ \omega: \qquad \textit{magnitude} \\ \angle g_{ij}(s) \mid_{s=j\omega}\ \text{versus}\ \log \\ \textit{omega}: \qquad \textit{phase} \end{array} \tag{28}$$

where $g_{ij}(s)$ denotes any of the transfer functions of Eq. (25). The left-hand side of the first of Eqs. (28) defines the magnitude in *decibels* (dB).

An Example. A simple classical design example will now be presented. The vehicle chosen is a jet-powered transport similar to that shown in Fig. 4. A single flight condition consisting of cruising flight at Mach 0.84 and altitude 33,000 ft has been chosen for study. Only longitudinal motion will be examined, and the control inputs will be the elevator angle $\Delta\delta_e$ and engine thrust $\Delta\delta_T$. The synthesis tools to be employed can be found in any undergraduate text on the subject, for example, Nise (9). Table 1 lists the stability derivatives for this flight condition. Referring to Eqs. (19), any stability derivatives appearing in the equations but absent from Table 1 are assumed negligible. The flight control system will be designed for use as an autopilot, that is, the only pilot inputs allowed will be commanded changes in the reference airspeed and altitude. The resulting flight control system, referred to as an *altitude–airspeed hold* system, is an autopilot found in all modern transport aircraft. Here the altitude variable *h(t)* is defined as

$$h(t) = z_0' - z'(t) \tag{29}$$

where z_0' represents the z' coordinate of the aircraft center of mass in the equilibrium condition.

The inner- and outer-loop control-system performance requirements are stated in terms of desired closed-loop *bandwidths*. Now a more precise definition of bandwidth can be offered. In control-system parlance, the bandwidth is typically defined as that frequency where the magnitude portion of the Bode plot of a closed-loop transfer function crosses and remains below the −3 dB line. For this design, the desired bandwidths are:

(1) Pitch-attitude (inner-loop) bandwidth: $2.0 \leq \omega_{\theta BW} \leq 4.0$ rad/*s*
(2) Altitude-rate (intermediate-loop) bandwidth: $0.5 \leq \omega_{hBW} \leq 1.0$ rad/s
(3) Altitude (outer-loop) bandwidth: $0.25 \leq \omega_{hBW} \leq 0.5$ rad/s
(4) Airspeed (outer-loop) bandwidth: $0.25 \leq \omega_{uBW} \leq 0.5$ rad/s

Control System Architecture. The flight control architecture is shown in Fig. 6. Of particular interest here is the nested loop structure mentioned in the preceding. Here, the innermost feedback loop involves

Table 1: Stability Derivatives for Example Aircraft[a]

$X_u =$	$-0.014\ \mathrm{s}^{-1}$	$X_w =$	$0.0043\ \mathrm{s}^{-1}$
$X_{\Delta\delta_e} =$	$0\ \mathrm{ft}\cdot\mathrm{s}^{-2}\cdot\mathrm{rad}^{-1}$	$X_{\Delta\delta_T} =$	$0.00014\ \mathrm{ft}\cdot\mathrm{lbf}^{-1}\cdot\mathrm{s}^{-2}$
$Z_u =$	$-0.0735\ \mathrm{s}^{-1}$	$Z_{\dot{w}} =$	0
$Z_w =$	$-0.806\ \mathrm{s}^{-1}$	$Z_{\Delta\delta_e} =$	$-34.6\ \mathrm{ft}\cdot\mathrm{s}^{-2}\cdot\mathrm{rad}^{-1}$
$M_u =$	$-0.000786\ \mathrm{s}^{-1}\cdot\mathrm{ft}^{-1}$	$M_{\dot{w}} =$	$-0.00051\ \mathrm{ft}^{-1}$
$M_w =$	$-0.0111\ \mathrm{s}^{-1}\cdot\mathrm{ft}^{-1}$	$M_q =$	$-0.924\ \mathrm{s}^{-1}$
$M_{\Delta\delta_e} =$	$-4.59\ \mathrm{s}^{-2}$	$u_0 =$	$824.2\ \mathrm{ft}\cdot\mathrm{s}^{-1}$

[a]Flight condition: Mach 0.84, altitude 33,000 ft.

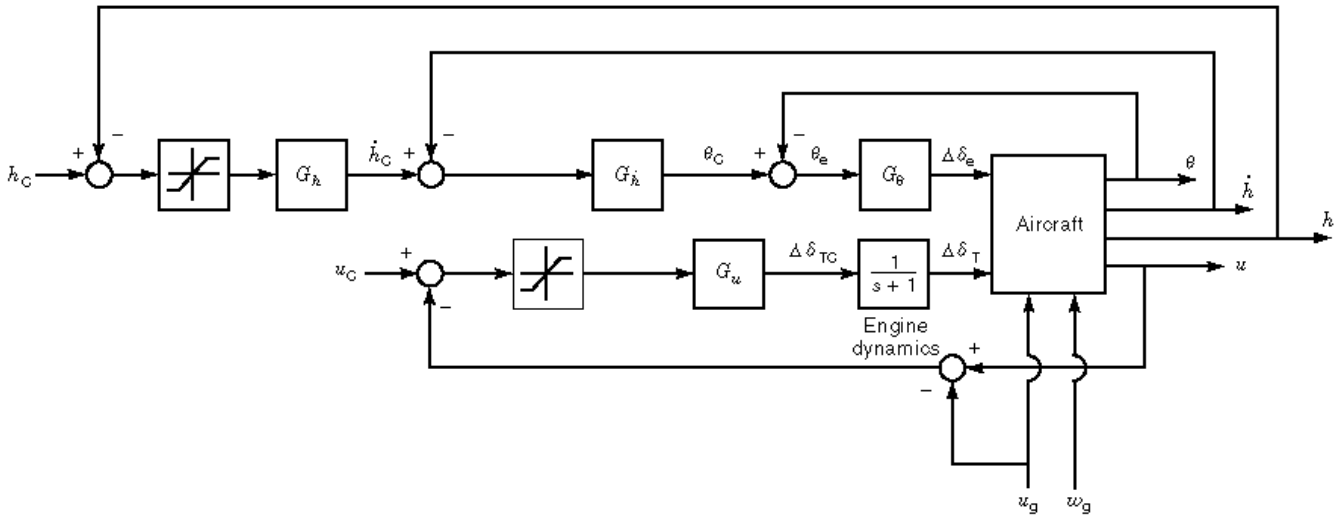

Fig. 6. Flight control system for the example.

feedback of pitch attitude θ with the elevator serving as the control effector. The error $\theta_c - \theta$ serves as an input to the pitch *compensation element* G_θ. The pitch-attitude command θ_c is the output of the altitude-rate compensation element $G_{\dot{h}}$ that receives the error signal $\dot{h}_c - \dot{h}$ as its input. In turn, the altitude-rate command is the output of the altitude compensation element G_h that receives the error signal $h_c - h$ as its input. Finally, an airspeed loop is incorporated, involving feedback of airspeed perturbation (including turbulence) $u - u_g$ with engine thrust serving as the control effector.

A simple engine model is employed as

$$\frac{\Delta\delta_T}{\Delta\delta_{T_c}} = \frac{1}{s+1} \quad \frac{(\text{lbf thrust})}{(\text{lbf thrust command})} \tag{30}$$

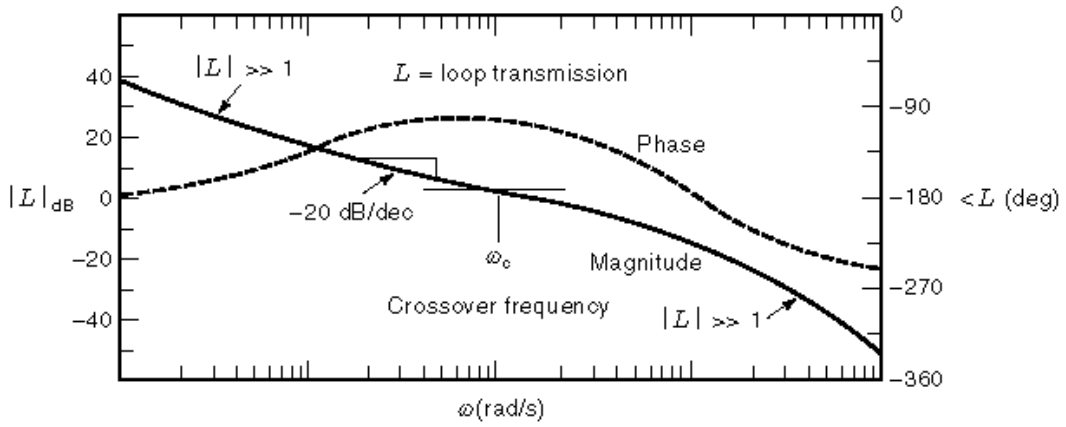

Fig. 7. Attributes of a desirable loop transmission.

The representation of Eq. (30) is included to model the response lag between thrust commands and thrust output that occurs in a jet engine . Although simple in form, the first-order lag can often suffice for such designs [see, for example, Stevens and Lewis, (11, Chap. 3)].

Obviously, more complex models can be utilized. The dynamics of the actuation devices that drive the control effectors have been neglected here for simplicity. Also note that limiters have been placed in the $\dot{h}$ and u loops. Such limiters are common in flight control system, to prevent control actuator saturation when large step changes in outer-loop command values occur. Finally, note that disturbance inputs in the form of turbulence perturbations u_g and w_g are included, as provided by Eq. (19). The sensor requirements for the control system of Fig. 6 are pitch attitude, vertical velocity or altitude rate, altitude, and airspeed, all assumed referenced to the equilibrium flight condition.

Design Procedure. The design of the flight control system consists in determining the transfer functions of the compensators G_θ, $G_{\dot{h}}$, G_h, and G_u so that the performance specifications given in the preceding are met. Classical *sequential loop-closure* and *frequency-domain loop shaping* (14) will be used to obtain these compensation elements. This time-honored technique consists in focusing upon one feedback loop at a time, beginning with the loop with the largest bandwidth requirement. Here, this is the pitch-attitude loop. The transfer function $\theta/\Delta\delta_e(s)$ is obtained from the transfer function matrix $\boldsymbol{G}(s)$ introduced in Eq. (25). The compensation element G_θ is obtained so that the resulting *loop-transmission* $L(j\omega) = \theta_e/\theta$, with θ_e and θ as in Fig. 6, exhibits the frequency-domain characteristics prescribed by the Bode plot shown in Fig. 7. A loop transmission exhibiting these characteristics can be shown to exhibit good command-following and disturbance rejection performance with a closed-loop bandwidth approximately equal to the *crossover frequency*. The crossover frequency is defined as the frequency ω_c where the magnitude of the loop transmission equals 0 dB (14). Table 2 shows the transfer function selected for G_θ. After G_θ has been obtained, the θ loop is closed analytically, and Fig. 8 results. The θ loop has now been subsumed into a new *effective* vehicle with θ_c and $\Delta\delta_T$ serving as inputs. The expression $\theta \rightarrow \Delta\delta_e$ appearing in Fig. 8 is shorthand notation to indicate that the effective vehicle now includes a feedback loop in which the pitch attitude θ is being controlled by the elevator input $\Delta\delta_e$. Modern computer-aided design tools enable the analyst to perform these loop closures with relative ease.

The loop with the next highest bandwidth requirement is now selected, here corresponding to the $\dot{h}$ loop. Once again, loop shaping is employed, with the loop transmission $\dot{h}_e/\dot{h}$ being forced to resemble the ideal loop transmission shown in Fig. 7. Table 2 shows the resulting transfer function $G\dot{h}$. Figure 9 shows the new effective vehicle, now with $\dot{h}_c$ and $\Delta\delta_T$ serving as inputs.

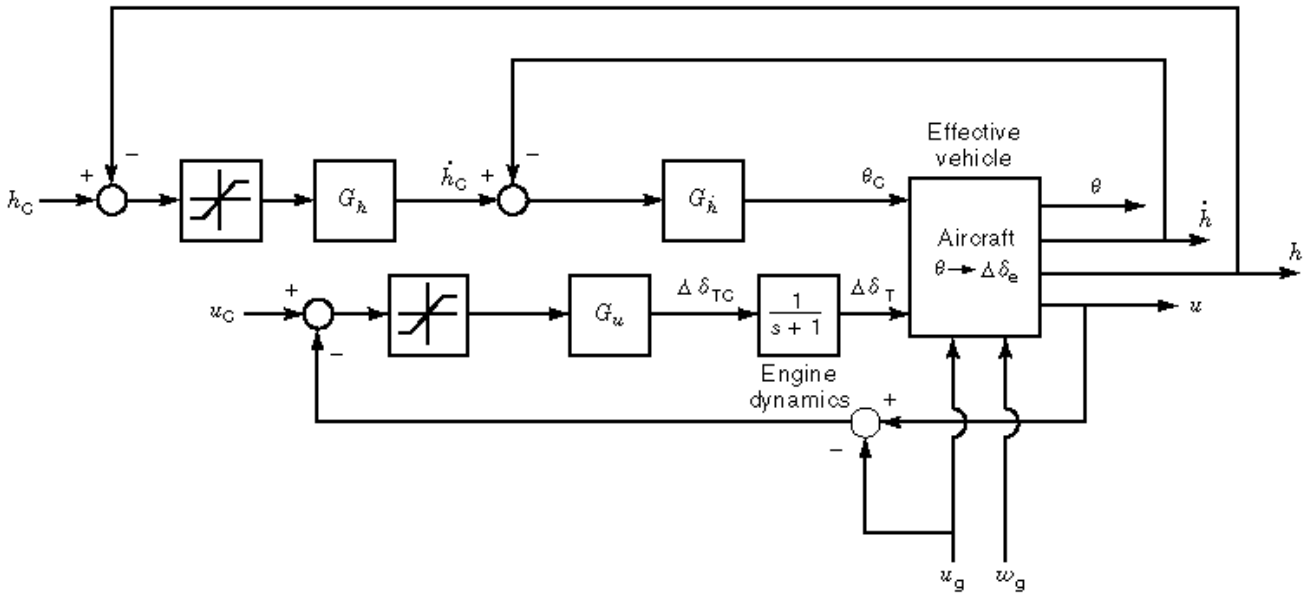

Fig. 8. Flight control system for the example, with pitch-attitude loop closed.

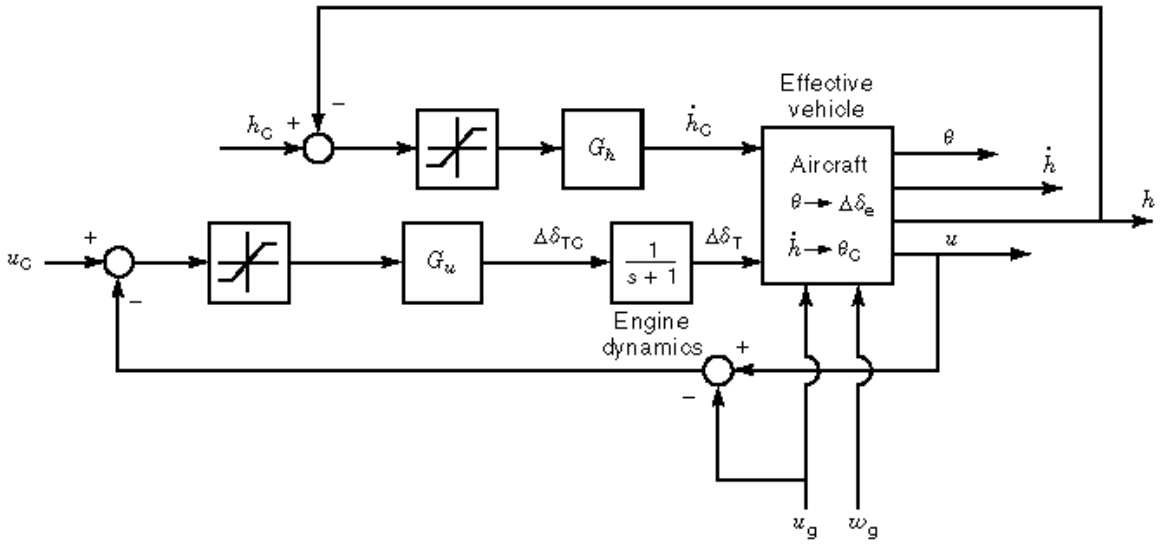

Fig. 9. Flight control system for the example, with pitch-attitude and altitude-rate loops closed.

In a similar manner, the final two loops of the control system are closed. Since the bandwidth requirements for the h and u loops are identical, either may be chosen first. Here, the h loop was selected, with the resulting G_h shown in Table 2. Figure 10 shows the resulting effective vehicle, with h_c and $\Delta\delta_T$ serving as inputs. Finally, the airspeed loop is closed with the G_u shown in Table 2. The final effective vehicle is shown in Fig. 11, now with h_c and u_c serving as inputs.

Table 2: Compensator Transfer Functions for Flight Control Example

$$G_\theta = -22.11\frac{(s^2+2.56s+10.24)(s+0.3)}{(s+0.015)(s+0.7)(s+20)^2} \text{ rad/(comand unit)}$$

$$G_{\dot{h}} = 0.03872\frac{(s+0.35)(s+0.5)}{s(s+10)} \text{ (ft/s)/(command unit)}$$

$$G_h = 0.233 \text{ ft/(command unit)}$$

$$G_u = 1780\frac{s+0.01}{s} \text{ (ft/s)/(command unit)}$$

$$G_1(z) = \frac{-0.001414z^6+0.004047z^5-0.003222z^4-0.001457z^3+0.004034z^2-0.002590z+0.0006021}{\Delta(z)}$$

$$G_2(z) = \frac{-0.006068z^6+0.01736z^5-0.01382z^4-0.006251z^3+0.01730z^2-0.01111z+0.002583}{\Delta(z)}$$

$$G_3(z) = \frac{-0.3179z^4+0.3379z^3+0.1406z^2-0.3479z+0.1674}{z^4-0.97819z-0.5535z^2+0.37942z+0.1535}$$

$$G_4(z) = \frac{1782z-1778}{z-1}$$

$$\Delta(z) = z^6-1.868z^5+0.2049z^4+0.9801z^3-0.1222z^2-0.1787z-0.01706$$

As one moves from inner to outer loops, the compensators become simpler in form, as the compensators of Table 1 indicate. The decreasing complexity in the compensation as one moves from inner to outer loops is an important result, since the quality (signal-to-noise ratios) of the sensed variables will generally be poorer as one moves to the outer loops. The decreasing compensator complexity is a direct consequence of the sequential loop closure procedure.

Digital Implementation of the Control Law. The compensator transfer functions $G_\theta(s)$, $G_{\dot{h}}(s)$, $G_h(s)$, and $G_u(s)$ of Table 2 constitute the flight control law for this application. As Fig. 2 indicates, such laws are now routinely implemented in a digital flight control computer. Thus, the control law must be expressed in a form suitable for digital implementation. To accomplish this, the nested control architecture of Fig. 6 is redrawn in an equivalent form where the compensators act in parallel. This can be easily done by referring to Fig. 6 and writing expression for the control inputs as

$$\begin{aligned}\Delta\delta_e &= G_\theta[G_{\dot{h}}(G_h(h_c-h)-\dot{h})-\theta] = G_1(h_c-h)-G_2\dot{h}-G_3\theta \\ \Delta\delta_T &= G_u[u_c-(u-u_g)] = G_4[u_c-(u-u_g)]\end{aligned} \tag{31}$$

Figure 12 shows the resulting control structure. The A/D and D/A blocks refer to *analog-to-digital* and *digital-to-analog* converters, respectively. "Analog" describes a continuous signal, and "digital" describes a discrete signal, that is, one that is a string of numbers. The sampling rate of the A/D devices is denoted by T, and the devices are assumed to operate synchronously. The means of accomplishing the continuous-to-discrete transformation is referred to as an *emulation method* (15, Chap. 5). In this method, the operation of the continuous compensators is approximated on the digital flight control computer by the *z-transfer functions*

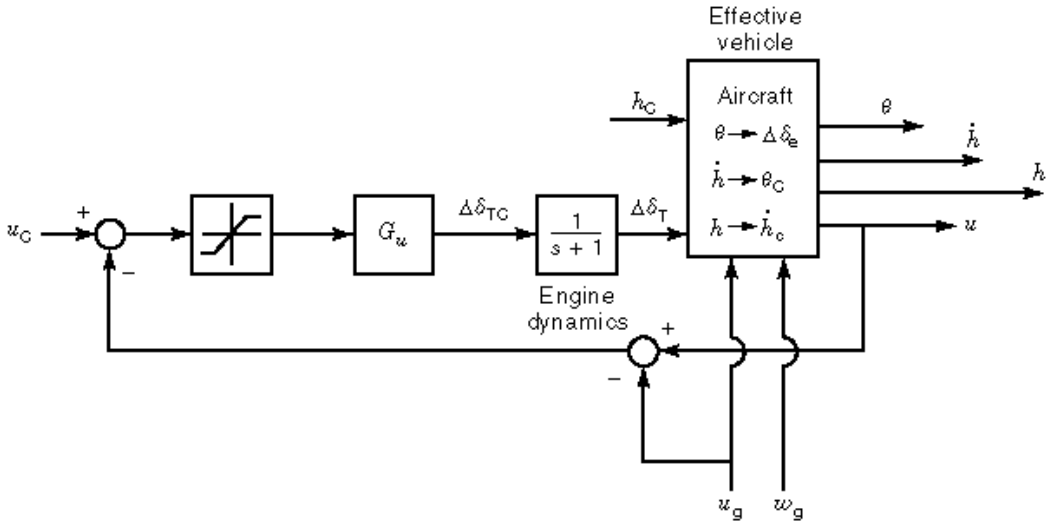

Fig. 10. Flight control system for the example, with pitch-attitude, altitude-rate, and altitude loops closed.

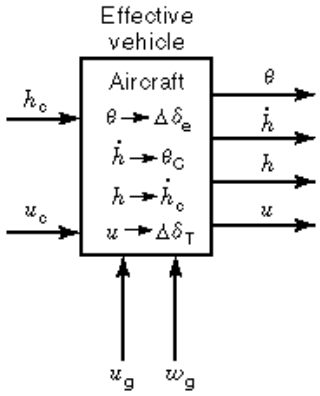

Fig. 11. Flight control system for the example, with all loops closed.

$G_i(z)$. A number of different emulation techniques exist, each dependent upon the type of discrete integration scheme that the digital computer uses to approximate the Laplace operator $1/s$. The most common of these is the bilinear (Tustin) transform (15). In this approach, the discrete transfer functions suitable for implementation on the digital flight control computer are obtained in the z domain. The *z transform* of a string of discrete numbers $x(kT)$ is defined as

$$X(z) = \sum_{k=-\infty}^{\infty} x(kT)z^{-k} \tag{32}$$

with the infinite sum on the right-hand side amenable to representation as a ratio of polynomials in z, much as the integral on the right-hand side of Eq. (24) is amenable to representation as a ratio of polynomials in the variable s.

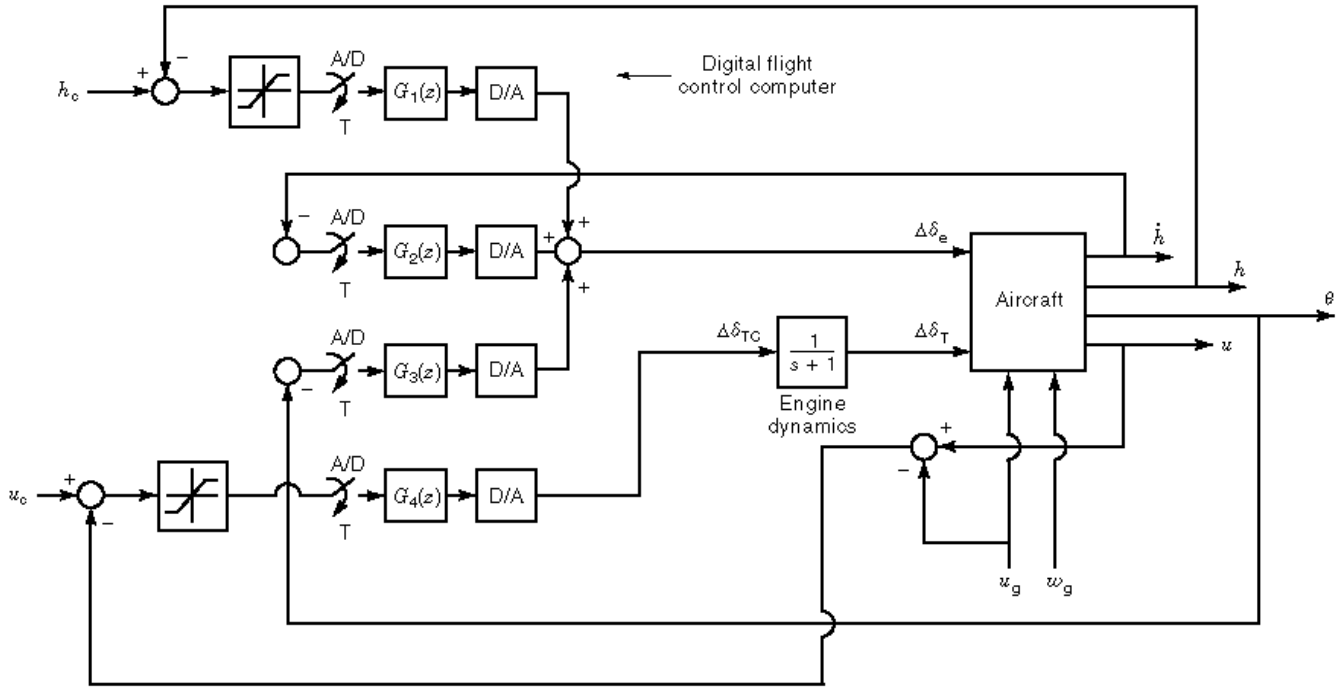

Fig. 12. Digital implementation of flight control law of the example.

The bilinear transformation is defined as

$$G(z) = G(s)\,|_{s=(2/T)(z-1)/(z+1)} \tag{33}$$

For the emulation method to provide control laws comparable to those obtained in a continuous system, the *sampling frequency* $\omega_s = 2\,\pi/T$ should be at least ten times the highest closed-loop bandwidth in the system (15). In the case of the flight control system designed here, the largest bandwidth is associated with the pitch-attitude loop. The bandwidth obtained with G_θ of Table 2 was approximately 2.5 rad/s. This requires that $\omega_s \geq 10 \times 2.5$ rad/s $= 25$ rad/s, or $T \leq 2\pi/\omega_s = 0.25$ s. This sampling interval is well within the capabilities of modern flight control computers. In Fig. 12, the elements $G_i(z)$ are defined as

$$\begin{aligned}
G_1(z) &= G_\theta(s)G_{\dot{h}}(s)G_h(s)\,|_{s=(2/T)(z-1)/(z+1)} \\
G_2(z) &= G_\theta(s)G_{\dot{h}}(s)\,|_{s=(2/T)(z-1)/(z+1)} \\
G_3(z) &= G_\theta(s)\,|_{s=(2/T)(z-1)/(z+1)} \\
G_4(z) &= G_u(s)\,|_{(2/T)(z-1)/(z+1)}
\end{aligned} \tag{34}$$

By writing the $G_i(z)$ in Eq. (33) in terms of inverse powers of z, *linear difference equations* can be formed between the input and output of each $G_i(z)$. These difference equations can then be programmed in the flight control computer. The last four rows of Table 2 give the $G_i(z)$ compensators with the sampling interval chosen as $T = 0.25$ s.

Performance Assessment via Simulation. Part of the design cycle of any flight control system involves computer simulation of the completed design with the control law implemented digitally. This simulation can involve any nonlinearities that may have been neglected in the synthesis procedure itself. In this case, the two limiters of Fig. 6 were included. To demonstrate the performance of the system just designed, a simulation run was conducted. This involved a commanded 1,000 ft increase in altitude from equilibrium value. In addition, at the initiation of the run, the aircraft encounters two simultaneous sharp-edge turbulence fields u_g and w_g, each of 20 ft/s. The command limiters in Fig. 6 were chosen with the following bounds: In the u loop, the limiter was selected with limits of ± 10 (command units)/(ft/s), while in the $\dot{h}$ loop the limits were ± 1000 (command units)/ft. The equilibrium point change involved a relatively minor flight-condition variation, so that the original aerodynamic model summarized in Table 1 was still valid for simulation purposes. Figures 13 and 14 show the airspeed, altitude, elevator, and thrust perturbation responses to the commands just described. Since no elevator actuator model was included, the effect of the D/A device is clearly evident in the $\Delta\delta_e$ time history. As the figures indicate, the equilibrium change was smooth, with no excessive elevator or thrust inputs.

Control-System Design—Modern Approaches

Limitations of Classical Sequential Loop Closure. The design of the previous section was successful, given the single flight condition, the limited number of control inputs considered, the relatively simple design specifications, the underlying assumption of linearity, and the inherent stability of the basic aircraft. Even with these assumptions, however, the ability to move from a set of performance specifications to a final control law is not straightforward and certainly not algorithmic. Success is highly dependent upon the skill and experience of the analyst.

Some modern flight control problems rarely allow the simplifications just enumerated. Consider the aircraft shown in Fig. 1. The absence of a vertical tail, dictated by a desire to minimize radar signature (i.e., to provide a *stealthy* design), means that at least one of the lateral directional modes of the vehicle will be unstable. To maximize maneuverability it is also likely that longitudinal modes will also exhibit instability. In addition, a wide variety of flight conditions will be contained within the aircraft's operational envelope. The use of the linear models in Eqs. (19) and (20) may not be justified in some flight regimes such as those in large-disturbance maneuvers. A large number of unconventional control effectors are also in evidence. Finally, in the event of combat damage, the control law may be required to be *reconfigurable*, that is, able to adapt to airframe damage by automatically restructuring itself.

These caveats are not meant to imply that sequential loop closure, per se, is not a useful approach to control system design. When taken as a part of more powerful design techniques, such as the quantitative feedback theory (*QFT*) approach to be discussed, sequential loop closure can be a powerful tool (16). Fortunately, advances in the theory of feedback control provide many synthesis tools that allow the flight control designer to attack the challenging problems just enumerated. An excellent and thorough summary of such techniques can be found in Ref. 17. An abbreviated review of a few of these techniques is provided next.

Linear Design Approaches.

Quantitative-Feedback-Theory Controllers. *QFT* describes a control-system design technique in which quantitative measures of aircraft stability and performance are guaranteed in the presence of *structured uncertainty* in the vehicle dynamic model. Such guaranteed stability and performance is referred to as *robustness*. Referring to the transfer function of Eq. (26), structured uncertainty is in evidence if the numerator and denominator coefficients are not known precisely, but can be assumed to lie between specific values. For example, it might be stated that the numerator coefficient a_i is known only to be in the interval $3.25 \leq a_i \leq 5.3$. This uncertainty may be attributable to errors in stability derivative estimates and/or to the changes in vehicle transfer functions that occur at different points in the flight envelope.

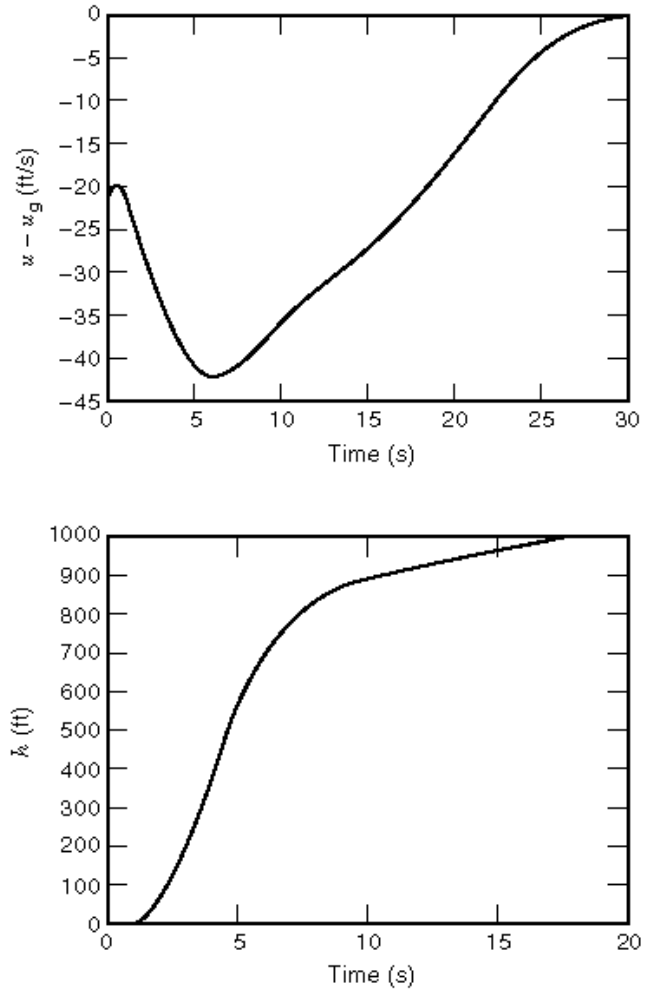

Fig. 13. Airspeed and altitude responses for the example.

In *QFT*, the desired control system performance is typically presented in terms of bounds on the allowable magnitudes of the Bode plots of system transfer functions across a frequency range of interest. *QFT* is a *frequency-domain*-based design technique. Thus the design is carried out on *Nichols charts* (9), in which the magnitude and phase of the system loop transmission are plotted and forced to lie above bounds dependent upon the desired stability and performance and the amount of uncertainty.

The attractiveness of *QFT* designs is their ability to handle structured uncertainty and to guarantee performance. In addition, the order of the controller is at the discretion of the designer. The primary disadvantage is that the technique is not algorithmic and, as yet, is not supported by widely available computer-aided design packages.

Linear Quadratic Regulator and Linear Quadratic Gaussian Controllers. A considerable number of control design techniques have been developed that derive from the minimization of *scalar norms*. Linear quadratic regulators (*LQR*s) fall into this category. Such designs seek a feedback control law of the form $\delta(t) = -\boldsymbol{K}\boldsymbol{x}(t)$, where $\boldsymbol{K}$ is a state feedback gain matrix. $\boldsymbol{K}$ is chosen to minimize a scalar norm or *performance index*,

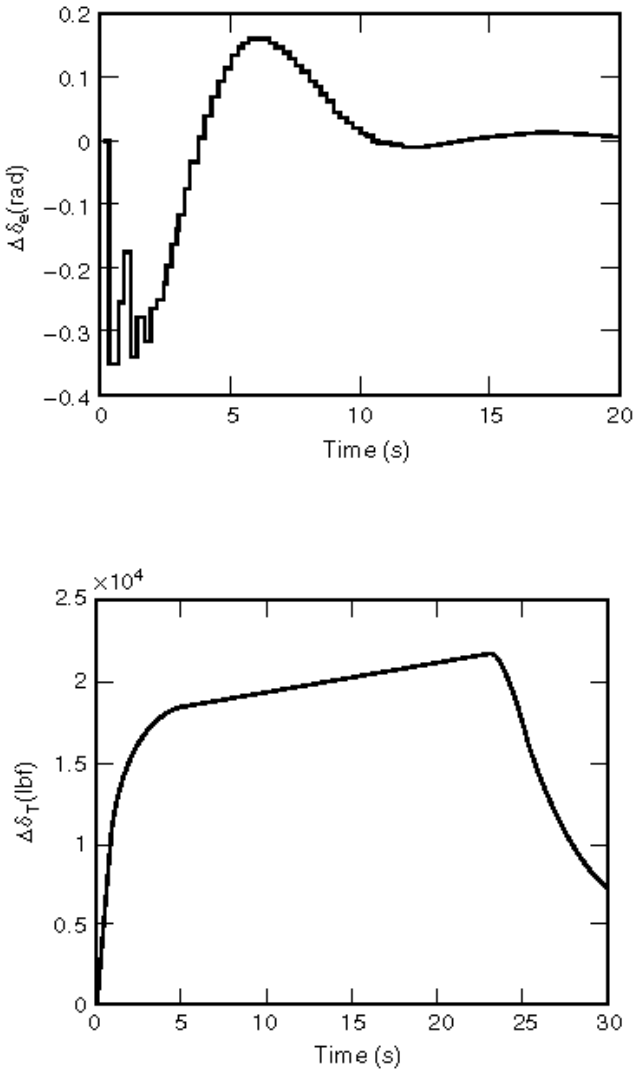

Fig. 14. Elevator and thrust responses for the example.

defined as a weighted sum of mean squared system errors and control inputs (sometime referred to as an L_2 norm). For example, one such index might be

$$J = \int_0^\infty [\boldsymbol{x}^{\mathrm{T}}(t)\,\boldsymbol{x}(t) + \boldsymbol{\delta}^{\mathrm{T}}(t)\,\boldsymbol{R}\boldsymbol{\delta}(t)]\,dt \tag{35}$$

Here the system error is defined as the deviation of the state vector $\boldsymbol{x}(t)$ from an equilibrium point. The solution to the *LQR* problem typically involves the solution of the matrix Riccati equation. As Eq. (35) indicates, implementation of such control laws requires measurement of the entire state vector. This requirement can be

obviated through introduction of a *state estimator* that provides continuous estimates of the state vector based upon measurement of a subset or combination of the system state variables.

If the aircraft is assumed to be disturbed by a random signal possessing a Gaussian amplitude distribution (e.g., random turbulence) and if the output variables are assumed corrupted by additive white noise, also possessing a Gaussian distribution, then linear quadratic Gaussian (*LQG*) controllers can be designed. As in the *LQR* controllers, the feedback gains for the *LQG* designs are obtained by solution of matrix Riccati equations. The state estimators in this designs are also optimal in the sense that a quadratic index of performance in minimized. The optimal estimators thus obtained are referred to as *Kalman filters*.

The attractiveness of *LQR* and *LQG* designs is their algorithmic nature and the fact that very efficient computer-aided design packages are available for their solution, e.g., the Matlab Control System Toolbox (18). Their primary disadvantage is that the designs are *regulators* and must be modified for use as command trackers.

H-Infinity Controllers. A system norm referred to as an *H-infinity* (H_∞) norm of a transfer function matrix $\boldsymbol{G}(s)$ can be defined as

$$[H_\infty \text{ norm of } \boldsymbol{G}(s)] = \|\boldsymbol{G}\|_\infty = \sup_\omega \sigma_{\max}[\boldsymbol{G}(j\omega)] \tag{36}$$

where the right-hand side refers to the least upper bound of the *maximum singular value* of $\boldsymbol{G}(j\omega)$ over all frequencies ω. Singular values (both maximum and minimum) extend the concept of a frequency-dependent gain from single transfer functions to matrix transfer functions. As in the case of the *LQR* and *LQG* controllers, finding H_∞ controllers involves the solution of matrix Riccati equations. One application of H_∞ could be the transport flight control problem considered earlier. By focusing upon the transfer-function matrix between the outputs $\theta(t)$, $z_0' - z'(t)$ and the turbulence inputs u_g, w_g [$\boldsymbol{H}(s)$ in Eq. (25)], one could seek the controller that minimized $\|\boldsymbol{H}\|_\infty$ and thus provide an efficient gust alleviation system.

As with *LQR* and *LQG* designs, the attractiveness in H_∞ controllers is the availability of efficient computer-aided design packages. In addition, the manner in which performance specifications can be couched in terms directly suitable to H_∞ formulations is desirable. The primary disadvantage of this design approach is that high-order controllers frequently result.

Eigenstructure Assignment. The roots of the denominator polynomials in a system transfer-function matrix such as $\boldsymbol{G}(s)$ in Eq. (26) are often referred to as system *eigenvalues*. The eigenvalues associated with the system before feedback is applied are referred to as open-loop eigenvalues, while those associated with the system after feedback is applied are referred to as closed-loop eigenvalues. *Eigenvectors* are column matrices, the elements of which describe the *mode shapes* of the vehicle responses. That is, the eigenvectors determine how each state variable contributes to the vehicle response for each possible mode of motion. Like eigenvalues, open-loop and closed-loop eigenvectors can be defined.

As a control-system design technique, eigenstructure assignment allows the creation of controllers that meet *mode-based* performance specifications. Examples of mode-based specifications are minimum damping, minimum settling time, and decoupled responses. The last refers to allowing specified system inputs to affect only certain system outputs. For example, in the case of the fighter aircraft of Fig. 1, it may be desirable to have the elevons affect only pitching motion, while the spoilers affect only vertical velocity.

One of the attractive features of eigenstructure assignment for the control of piloted aircraft is the manner in which design criteria for handling qualities can be directly incorporated into the mode-based controller specifications. In addition, the order of the compensator is at the discretion of the designer. Possible disadvantages of this approach include the difficulty in determining how to tune an eigenstructure assignment design (improve its performance) if its performance in simulation or flight is unsatisfactory.

Model-Following Controllers. As the name implies, model-following controllers involve control structures in which the vehicle's response is forced to follow that of an ideal or desired model. Model-following

designs are usually described as either *explicit* or *implicit*. In explicit model following, a model of the desirable vehicle dynamics appears explicitly in a feedforward path. This is sometimes referred to as model-in-the-system control. Errors between the model response and that of the vehicle are used to create control inputs. In implicit model following, sometimes referred to as model-in-the-performance-index control, no model appears explicitly. In one type, the model influences the control strategy through its appearance in a quadratic performance index like that given in Eq. (35).

Model-following control structures are also used in research aircraft that serve as *in-flight simulators*. Here the dynamics of the vehicle being simulated form the model. A historical review of in-flight simulation can be found in Gowran and Reynolds (19).

Like eigenstructure assignment, model following is an attractive control strategy for piloted aircraft, since handling-qualities criteria can be used to select the ideal model. Possible disadvantages include large-bandwidth requirements associated with obtaining high-fidelity model-following characteristics.

Nonlinear Design Approaches.

Nonlinear Dynamic Inversion (Feedback Linearization) Controllers. *Nonlinear dynamic inversion* or *feedback linearization* refers to a control-system design approach in which the aircraft's nonlinear response characteristics are dynamically linearized through a state feedback law. The word "dynamically" is used here to differentiate this approach from the small-disturbance linearization discussed earlier. Like *LQR* and *LQG* approaches, dynamic inversion requires full state feedback or state estimation.

Dynamic inversion is attractive in that it is applicable to flight regimes in which nonlinearities cannot be ignored or eliminated through small-disturbance theory. More than any competing nonlinear approaches, these controllers have been successfully flight-tested on a number of aircraft, including helicopters (20).

The primary disadvantages revolve around the aforementioned full-state-feedback requirement and the fact that systems possessing *transmission zeros* in the right half of the complex s plane (so-called *non-minimum-phase* characteristics) cannot be accommodated without considerable difficulty. Transmission zeros represent an extension of the concept of zeros of a single transfer functions to those of a transfer function matrix (14). The solution to the problem of non-minimum-phase transmission zeros often requires the introduction of *regulated* response variables. An additional disadvantage of course, is that, a detailed model of the nonlinear vehicle is required.

Sliding Mode Controllers (Variable-Structure Controllers). Sliding mode control is a design technique that begins with the definition of the n system state variables. Then a *sliding surface* is defined in the $(n + 1)$-dimensional space (time included). The surface is defined so that if the system state trajectory remains on (slides on) this surface, desirable system behavior such as command tracking occurs. After design of the surface, a switching controller is constructed. If the trajectory moves off the sliding surface due to disturbances or tracking errors, the control inputs are created that point the tangents to the state trajectory back toward the surface. The state-space description of the system need not be linear in this approach.

The control action in sliding mode controllers is discontinuous and ideally requires infinitely fast switching mechanisms. Since such mechanisms are obviously unattainable, finite switching is employed. This leads to a phenomenon known as *chattering*, in which the control switches rapidly from one value to another. In aircraft control applications, chattering could excite unmodeled aeroelastic modes. To prevent chattering, a thin *boundary layer* surrounding the sliding surface is introduced so that when the state trajectory enters the layer, the control changes are smooth.

Like dynamic inversion, the attractiveness of sliding mode controllers lies in their applicability to nonlinear systems. Unlike dynamic inversion, sliding mode controllers are not limited to systems possessing minimum-phase transmission zeros. Possible disadvantages include the necessity of specifying the thickness of the sliding surface boundary layer and the modifications of the control law when the state trajectory enters the layer.

Neural-Net Controllers. Neural-net controllers utilize artificial *neural networks* that emulate the low-level biological functions of the brain to solve difficult control problems. Essentially, neural nets provide a

means for mapping the input–output characteristics of complex nonlinear systems. As such, they are useful for nonlinear flight control problems. As opposed to being analytically designed, neural nets are *trained* to model vehicle nonlinear dynamics. Once trained, they can then be incorporated into a control system, for example as part of a nonlinear dynamic inversion controller (e.g., Ref. 21). Given a nonlinear model of the aircraft, the net is trained to invert the system dynamics for a variety of desired outputs, that is, to determine the control inputs which provide the desired outputs. The trained net then is used online as a controller. To minimize the effects of errors in the net operation, other loops are closed around the neural-net dynamic inverter. In Ref. 21 this involved an adaptive system using a second neural-net controller.

The attractiveness of neural-net controllers lies in their ability to serve as nonlinear controllers when tractable analytical models of system nonlinearities are unavailable. Disadvantages that are often cited include the need to determine whether the net has been sufficiently trained and to establish the structure of the net itself.

Adaptive Control. *Adaptive control* refers to a class of controllers that can alter their parameters or structures in response to unpredicted changes in the vehicle and/or environment. The term "unpredicted" distinguishes adaptive control from other forms of controller on-line modification such as that employed in *gain scheduling*. The latter refers to designing controllers for known, fixed points (or equilibrium conditions) and then blending the controller parameters as the equilibrium point changes. Gain scheduling is widely used in aircraft flight control, where the scheduling is based upon sensed changes in altitude and Mach number.

Adaptive controllers are often referred to as *self-tuning*, *self-optimizing*, and *self-learning*. *Model-reference adaptive control* is an approach in which errors between vehicle outputs and those of an ideal model are employed in online adjustment of controller parameters. In other adaptive algorithms, the process of adaptation often involves *system identification*, wherein models of the vehicle are derived online, in real time.

Aircraft applications of adaptive control are challenging in that the adaptation process as a whole must occur very quickly. For example, one of the most challenging current applications of adaptive control lies in the area of *reconfigurable flight control*. Here, the controller is required to adapt to damage to the aircraft or to subsystem failures. In the case of combat aircraft such as that of Fig. 1, wherein vehicle stability is dependent upon active feedback control, damage or subsystem failures can easily cause the vehicle to become uncontrollable by the pilot in a matter of seconds or less. As an example, Bodson and Groszkiewicz (22) offer a treatment of this problem using model-reference approaches.

The attractiveness of adaptive control is its promise of providing control laws for aircraft applications in which significant and unpredictable changes in vehicle characteristics may occur. Disadvantages often concern stability guarantees and the complexity of the controllers themselves.

BIBLIOGRAPHY

1. B. Etkin *Dynamics of Flight—Stability and Control*, 2nd ed., New York: Wiley, 1982.
2. R. C. Nelson *Flight Stability and Automatic Control*, 2nd ed., New York: McGraw-Hill, 1998.
3. L. V. Schmidt *Introduction to Aircraft Flight Dynamics*, AIAA Education Series, Reston, VA: American Institute of Aeronautics and Astronautics, 1998.
4. R. A. Hess Stability and turbulence, in R. C. Dorf (ed.), *The Engineering Handbook*, Boca Raton, FL: CRC Press, 1996, Chap. 173.
5. D. T. McRuer I. Ashkenas D. Graham *Aircraft Dynamics and Automatic Control*, Princeton, NJ: Princeton University Press, 1973.
6. R. K. Heffley *et al. A Compilation and Analysis of Helicopter Handling Qualities Data, Vol. 1: Data Compilation*, NASA CR-3144, 1979.
7. M. B. Tischler (ed.) *Advances in Aircraft Flight Control*, London: Taylor and Francis, 1996.
8. M. Waszak D. K. Schmidt Flight dynamics of aeroelastic vehicles, *J. Aircraft*, **25** (6): 563–571, 1988.
9. N. S. Nise *Control Systems Engineering*, 2nd ed., Menlo Park, CA: Addison-Wesley, 1995.

10. G. E. Cooper R. P. Harper, Jr. The use of pilot rating in the evaluation of aircraft handling qualities, NASA TN D-5153, 1969.
11. B. L. Stevens F. L. Lewis *Aircraft Control and Simulation*, New York: Wiley, 1992.
12. A. E. Bryson Y. C. Ho *Applied Optimal Control*, New York: Hemisphere, 1975.
13. R. F. Stengel *Stochastic Optimal Control, Theory and Applications*, New York: Wiley, 1986.
14. J. M. Maciejowski *Multivariable Feedback Design*, Menlo Park, CA: Addison-Wesley, 138–142, 1989.
15. G. F. Franklin J. D. Powell M. L. Workman *Digital Control of Dynamic Systems*, 2nd ed., New York: Addison-Wesley, 1990.
16. P. J. Gorder R. A. Hess Sequential loop closure in design of a robust rotorcraft flight control system, *J. Guidance Control Dynamics*, **20** (6): 1235-1240, 1997.
17. W. S. Levine, ed. *The Control Handbook*, Boca Raton, FL: CRC Press, 1996.
18. Anon., *Control System Toolbox User's Guide*, Natick, MA: MathWorks, Inc., 1998.
19. V. J. Gowran P. A. Reynolds When in-flight simulation is necessary, *J. Aircraft*, **32** (1): 411–415, 1995.
20. G. A. Smith G. Meyer Aircraft automatic flight control system with model inversion, *J. Guidance Control Dynamics*, **10** (3): 269–275, 1987.
21. B. S. Kim A. J. Calise Nonlinear flight control using neural networks, *J. Guidance Control Dynamics*, **20** (1): 26–33, 1997.
22. M. Bodson J. E. Groszkiewicz Multivariable adaptive algorithms for reconfigurable flight control, *IEEE Trans. Control Syst. Technol.*, **5** (2): 217–229, 1997.

RONALD A. HESS
University of California